Curving Around Obstacles via NN-Enabled Wavefront Shaping in Sub-THz Wireless Networks

Haoze Chen, Atsutse Kludze, Yasaman Ghasempour
Department of Electrical and Computer Engineering, Princeton University, Princeton, NJ 08544 USA
Email: {hc9271, kludze, ghasempour}@princeton.edu

GLOBECOM 2024 - 2024 IEEE Global Communications Conference | 979-8-3503-5125-5/24/$31.00 ©2024 IEEE | DOI: 10.1109/GLOBECOM52923.2024.10901766

***Abstract*—The sub-THz band offers an attractive solution to future wireless networks, thanks to its ultra-low latency as well as its large available bandwidth. However, link blockage remains a major setback towards reliable sub-THz end-to-end communication systems, due to narrow beamwidth and inherently high penetration losses. To achieve blockage mitigation in sub-THz communication, this paper takes advantage of unique near-field properties and manipulates curved wavefront trajectories. Unfortunately, finding the best curved beam configuration is non-trivial due to the lack of a closed-form equation for received power calculation under blockage scenarios, even if the wireless environment is precisely known. To address this, we present a physics-informed learning-based framework that optimizes the phase profile of the transmitting array, such that the resulting wavefront could curve around obstacles and adapt to dynamic environments in real time. Through extensive near-field simulations, we evaluate the performance of our AI-generated curved beams as opposed to optimal Airy beams achieved via impractical exhaustive scans with prohibitively large time and complexity overheads. Importantly, simulated results show that our AI-generated curved wavefront provides an average SNR gain of 19.83 dB compared with conventional beam steering and 2.13 dB compared with near-field beam focusing, across ~ 400 random and independent test scenarios.**

***Index Terms*—Sub-THz, Airy Beam, Near Field Propagation, Wavefront Engineering, Physics-Informed Neural Network**

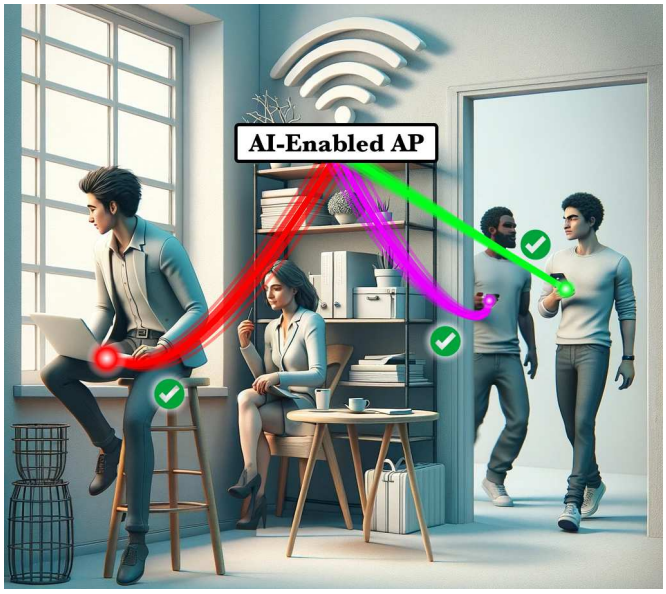

Fig. 1: Real-time adaptation of curved wavefront trajectories for blockage mitigation via an AI-empowered access point.

I. Introduction

Sub-Terahertz wireless systems are emerging due to their exceptional potential in communication and sensing, owing to their large available bandwidth and ultra-low latency [1]–[4]. However, the main bottleneck of such systems is susceptibility to blockage as penetration losses increase at higher frequencies [5]. There exist several blockage mitigation techniques in the literature that rely on the presence of alternative link paths (strong reflection or other nearby access points) [6], [7]. Unfortunately, such alternative paths may not be present in many environments. Hence, this paper focuses on a new solution that does not assume alternative paths, but instead leverages the near-field channels that are prevalent at sub-THz regimes, e.g., the radiative near-field range extends to $\sim$ 7m with a 10cm transmitting aperture at 100 GHz.

In particular, in near-field regions, we can create complex wavefronts with interesting properties [8]. In this work, we focus on Airy beams, a wavefront in which its main lobe follows a curved trajectory in free space. We aim to use this intriguing property to "curve" around obstacles, realizing blockage avoidance and mitigation in sub-THz wireless networks as shown in Fig. 1. While preliminary studies have shown that such curved beams can indeed enhance the SNR of blocked users [9], finding the best wavefront configuration (i.e., curved trajectory) remains a challenge. Specifically, the optimal wavefront is a complicated function of both the environment (i.e., blocker) and the topological properties of communication parties. Evidently, an exhaustive search over all possible curved beam configurations is not feasible.

In this paper, we propose a physics-informed learning-based framework that finds the optimal curved beam that maximizes the power at the receiver under arbitrary obstruction. The key idea is that by adopting a one-time pre-trained neural network (NN), the transmitter can adapt its wavefront to dynamic environments with minimal computational and time overhead. In particular, according to the physics of Airy beams, we first uniquely characterize a curved beam with three independent variables, i.e., focal length, steering angle, and curvature coefficient, such that the exact trajectory is a non-linear and complex function of all three parameters. We also abstract a blocker via its size and location features. We conduct extensive

This work is supported in part by the National Science Foundation (grant CNS-2148271), the Air Force Office of Scientific Research (grant FA9550-24-1-0144), and in part by the Qualcomm Innovation Fellowship.

near-field EM simulations considering more than 1800 random environments and receiver locations, and run exhaustive scans to find the true-optimal curved beam parameters. We use this dataset to train a physics-informed neural network (NN) that maps a given environmental input to the optimal three-variable curved beam configuration. We envision that such an AI-based wavefront shaping framework can enable real-time adaptation of transmitted wavefront trajectories to user or environmental mobility, without incurring the prohibitive overhead of full-wave simulations or a brute force wavefront search.

The key contributions of this work are as follows:

- The first framework to shape curved beams for blockage mitigation in sub-THz wireless networks.
- An extensive dataset covering the true-optimal curved beam configurations in random blockage scenarios, each solution exhaustively searched using the iterative Rayleigh-Sommerfeld Integral.[1]
- A systematic evaluation of the ability of curved beams to reduce blind spots or shadow areas.
- A physics-informed neural network for curved wavefront optimization, achieving an average gain of 19.83 dB over conventional Gaussian beam steering, and 2.13 dB compared to near-field beam focusing. Further, the average performance loss of our NN-enabled wavefront shaping is less than 0.8 dB compared with an impractical exhaustive wavefront search.

II. Obstacle Avoidance with Curved Beams

In this paper, we focus on a particular near-field sub-THz wavefront, the *Airy beam*[2], due to its intriguing potential for blockage aviodance [9]. In the near field region, the Airy wavefront is both self-accelerating (its main lobe follows a curved trajectory in free space) and non-diffracting (it does not spread out like ordinary spherical waves). Its ideal 2D electric field profile can be modeled as:

$$E(y,x) = Ai(\sqrt{B_o k}y \ - \frac{x^2}{4B_o}) e^{i(\sqrt{\frac{k}{4B_o}}yx - \frac{1}{12}(\frac{x}{B_o})^3)}, \quad (1)$$

where $Ai(\cdot)$ is the Airy function, k is the wave number, y and x are transverse and propagation directions respectively, and B_o is a scalar parameter. The term $\frac{x^2}{B_o}$ describes the wave's trajectory which implies that the parabolic trajectory of the Airy beam can be adjusted with parameter B_o to transmit around an obstacle.

In this paper, we limit the Airy curvature to a 2D plane, where a 2D obstruction is considered. We note that 3D obstacles can be treated in a similar fashion by considering and comparing optimal beams living within multiple rotated 2D planes that contain both the transmitter and the receiver. We leave the extension to 3D for future work.

A. Principles of Curved Beam Generation

Curved beams can be generated following conventional beamforming and the principle of Fourier optics [11]. Indeed, a curved beam can be uniquely characterized with three parameters: *(i)* the steering angle θ relative to the transmitter; *(ii)* the focal length f; and *(iii)* the curvature coefficient B. Interestingly, we can decompose the overall phase profile into phase patterns needed for steering, focusing, and curving:

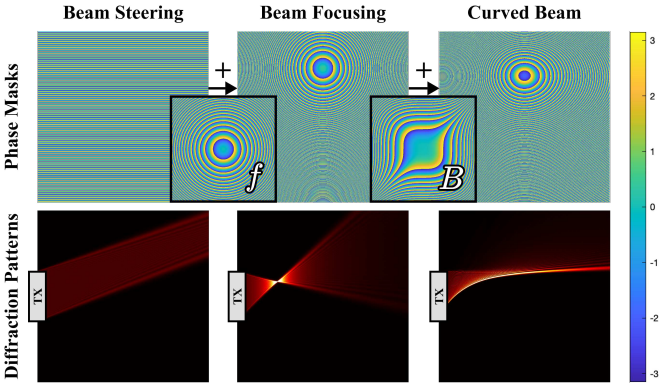

Fig. 2: Curved beam generation and parameterization.

First, the phase front at the transmit array needed to realize a wavefront steering angle of θ can be written as:

$$\phi_{steer}(y,\theta) = -k_o(y - \frac{D}{2})\sin\theta, \quad (2)$$

where D is the linear dimension of the array, and k_o is the free space wave number. Next, we apply an additional phase profile to realize the properties of beam focusing using paraxial approximation [12]:

$$\phi_{BF}(y,f) = -k_o\frac{y^2}{f}, \quad (3)$$

where f is the focal length, the absolute distance from the center of the array to the point of focus. This phase profile is crucial to the generation of Airy beams as it enables a fundamental principle in Fourier optics: if an additional phase profile is applied in conjunction with Eq. (3), the resulting E-field at the set focal length will be the Fourier transformation of that phase profile. Following this, we apply a cubic phase on top of Eq. (3), defined as:

$$\phi_{cubic}(y,B) = \frac{(2\pi By)^3}{3}, \quad (4)$$

such that its Fourier transformation becomes a scaled Airy function $\frac{1}{B}Ai(\frac{y'}{B})$ [13]. Based on its physical effect on the curving trajectory, we define B as the curvature coefficient. Hence, given the Fourier optics principle, we can write the overall desired phase to generate this curved beam as:

$$\phi_{curve}(y,\theta,f,B) = \phi_{steer}(y,\theta) + \phi_{BF}(y,f) + \phi_{cubic}(y,B)$$

Fig. 2 shows the individual contribution of each of these phase fronts. In this work, we take advantage of this generation process to realize arbitrarily curved beams and to uniquely parameterize curved beams with $\{B, f, \theta\}$.

[1]Dataset and pre-trained NN parameters are available through [10].

[2]We use "Airy beam" and "curved beam" interchangeably in this paper.

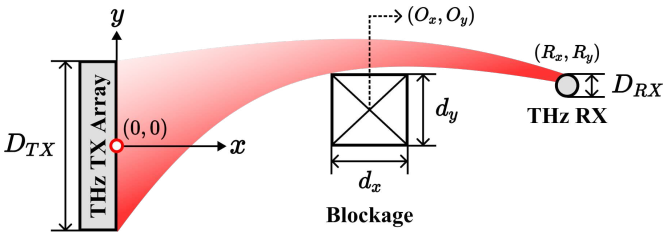

Fig. 3: System model and environment abstraction.

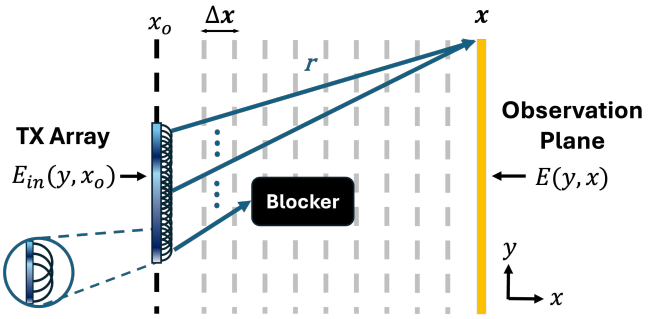

Fig. 4: Demonstrating the Rayleigh-Sommerfeld integral under an arbitrary E-field distribution and the presence of a blocker.

B. System Model

We consider a 2D indoor sub-THz communication system at 100 GHz[3] as shown in Fig. 3, where the transmitting array has a fixed location and aperture length of D_{TX}. The x axis represents the propagation direction while the y axis represents the transverse direction. The transmitter creates an Airy beam to curve around a rectangular-shaped obstacle with location (O_x, O_y) and dimensions (d_x, d_y), along the x and y axes, respectively. Finally, the receiver is located at (R_x, R_y) and has a fixed aperture size of D_{RX}.

It is evident that the curved wavefront should be configured and adapted based on the location of the mobile receiver and the dynamics of the environment (i.e., geometric features of the blocker). In this work, we assume that the perfect knowledge of the receiver's location and the blocker's information is available at the transmitter (e.g., via conventional perception techniques such as computer vision and radar)[4]. Hence, our goal is to find the optimal Airy parameters that achieve the maximum received power under the given environment. We can formulate our optimization goal as:

$$\{B^\star, f^\star, \theta^\star\} = \underset{\{B,f,\theta\}}{\arg\max}\, P_{RX}(B, f, \theta, O_x, O_y, d_x, d_y, R_x, R_y), \tag{5}$$

where $P_{RX}(\cdot)$ denotes the received power. Unfortunately, finding the optimal wavefront faces multiple challenges:

First, unlike far-field communication where the propagation loss (in free space and the case of shadowing) is well understood and modeled, near-field propagation lacks accurate channel models [14]. In particular, there is no closed-form equation that captures the received power under a given environment and a certain wavefront configuration. Consequently, conventional optimization techniques fail to solve Eq. (5) due to the unavailability of a closed-form objective function that maps Airy configurations to received powers (P_{RX}) under blockage.

Second, an exhaustive search over the entire parameter space is not feasible. In directional WLANs (e.g., IEEE 802.11ay [15]), it is common practice for the transmitter to scan all beam directions to find the maximum-power achieving beam for a directional point-to-point link. However, a similar exhaustive scan over a 3D space of $\{B, f, \theta\}$ incurs prohibitively large overhead and is not practical.

[3]The same principle applies to the entire sub-THz regime.

[4]We leave the exploration of semi-known environments for the future.

Lastly, we emphasize that in principle, the transmitter can perform full-wave analysis with EM solvers to find the received power under a given curved beam configuration. However, the computational complexity of such EM simulations is extensive; hence, performing exhaustive simulations over Airy configurations is even more computationally prohibitive for a practical AP or UE. Indeed, this highlights the need for an offline and low-cost solution for accurate and real-time wavefront adaptation. To tackle these challenges, we present the first AI-aided wavefront adaptation framework that provides an optimal Airy beam that curves around a known obstacle and maximizes the receiver power.

C. Complexity-Aware Accurate Near-Field Simulations

Forming a comprehensive dataset to train our neural network requires extensive simulations in different environments, user locations, and Airy parameters. Conventional EM simulation solvers or full-wave numerical methods are computationally intensive even when run on our 96-core server. Therefore, for large-scale data collection, we adopt scalar diffraction theory where we model EM waves as complex scalar quantities that only contain magnitude information, as opposed to the traditional modeling where EM waves are modeled as vectors with both magnitude and direction information.

In particular, we use the Rayleigh-Sommerfeld (RS) integral to model the propagation characteristics of our wavefronts along the plane of propagation. The Rayleigh-Sommerfield integral is a scalar wave approximation method that accurately models the propagation of arbitrary EM signals. It assumes that each point of the source (in this case our simulated array with a pre-determined phasefront) emits out spherical waves along the transverse direction and sums each of their contributions at each point in space, as shown in Fig. 4. The Rayleigh-Sommerfield integral makes no assumption of the initial E-field distribution. Thus, we can write the electric field at an arbitrary location of (y, x) given an input electric field column vector $E_{in}(y, x = x_o)$ as:

$$E_{RS}(y, x|E_{in}) = \int E_{in}(y', x_o)\frac{x}{2\pi r^2}e^{ikr}\left(\frac{1}{r} - ik\right)dy', \tag{6}$$

where x_o is the initial propagation coordinate, y' is the transverse coordinate on the input electric field, and $r =$

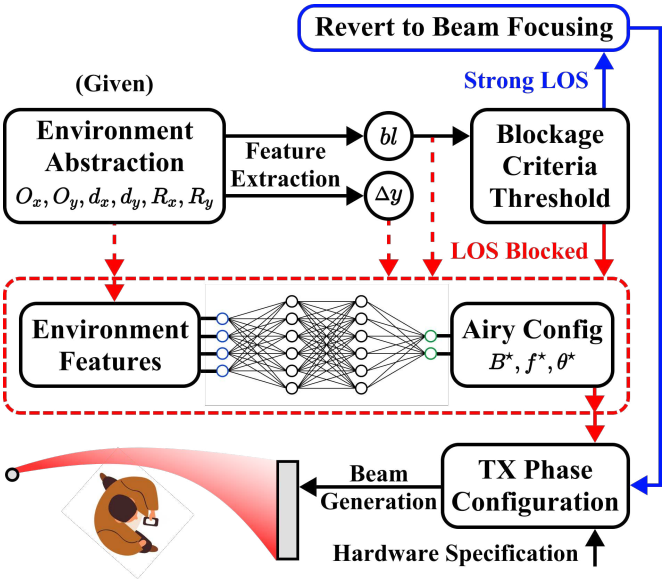

Fig. 5: An overview of our AI-generated airy wavefront.

$\sqrt{(x-x_o)^2+(y-y')^2}$.

Typically, Eq. (6) can calculate the E-field at any arbitrary distance away from the transmitter. However, in the presence of blockage, the normal diffraction behavior of the EM wave is disrupted. To account for this, Eq. (6) must be used iteratively along its propagation direction. Here, we introduce a binary matrix $OB(y,x)$, which takes the value of "0" if the blocker includes point (x,y) and takes "1" otherwise. Hence, we write the electric field distribution at the m^{th} iteration as

$$E_m(y,x) = OB(y,x)E_{RS}(y,x|E_{m-1}), \tag{7}$$

where $E_{m-1} = E(y, x = x_0 + (m-1)\Delta x)$ is a column vector representing the electric feature calculated from the previous step separated by distance Δx, as shown in Fig. 4. Please note that in the absence of blockage, $OB(y,x) = 1$, the iterative process of Eq. (7) yields the same result as Eq. (6).

III. Neural Network Enabled Wavefront Shaping

We present a physics-informed deep learning framework to optimize Airy configurations for blockage mitigation. Our high-level framework is shown in Fig. 5. If there exists a strong LOS path between the transmitter and receiver, our framework chooses to adopt a beam focusing wavefront. On the other hand, if no direct path can be found, we find an optimal curved beam by feeding the environmental features (e.g., blocker location) into a pre-trained physics-informed neural network. This neural network is trained using physical features of the environment along with ground truth optimal Airy configurations from exhaustive near-field wavefront search. With the optimal Airy beam parameters $\{B^\star, f^\star, \theta^\star\}$, we can construct a desired phase profile at the transmitter array (Sec. II-A). Taking hardware limitations into account, this phase profile can be quantized and re-optimized for practicality. Note that under dynamic channels, the curved wavefront should be adapted accordingly. Fortunately, the time and complexity overhead of such adaptation is minimal with a pre-trained NN.

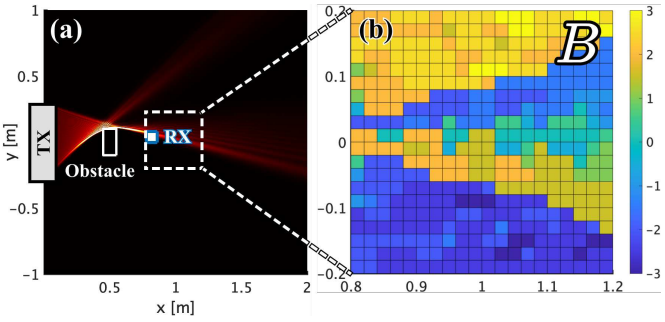

Fig. 6: (a) Moving RX within the shadow region behind an obstacle; (b) Optimal curvature B at each RX location.

A. Training Set Acquisition

We consider ~ 1500 random blockage settings to generate a comprehensive and representative training set, curated for our application. Specifically, we consider a transmit aperture of $D_{TX} = 60$cm, a receive aperture of $D_{RX} = 10$cm, and propagation distances up to 2m from the transmitter.[5] The receiver is moved within $R_x \in (0.6, 1.6) \wedge R_y \in (-0.8, 0.8)$ in meters, while the obstacle is placed randomly between the transmitter and receiver. The blocker size is set to be larger than 2cm (i.e., $7\times$ wavelength at 100 GHz) and smaller than 30cm (i.e., half as large as the transmitter aperture) to capture blockage cases feasible for Airy curving. We note that all parameters are sampled from uniform distributions across their corresponding ranges, putting together a random but representative dataset for blocked channel conditions. Further, to fit our application as shown in Fig. 5, we only take into account blockage settings in which the LOS path is at least partially blocked (i.e., scenarios that would activate Airy optimization). Indeed, if there is no blockage, a curved beam would not be needed. Moreover, we exhaustively go through the entire Airy configuration space $\{B, f, \theta\}$ to find the ground truth optimal Airy configuration that gives the maximum received power under each randomly generated environment.[6] Finally, for comparison purposes, we find the received power under near-field beam focusing for each setting. We note that the phase profile of beam focusing is determined only by the location of the receiver, i.e., a focal length of $f_D = \sqrt{R_x^2 + R_y^2}$ and a beam steering angle of $\theta_D = \arctan\frac{R_y}{R_x}$, regardless of blockers in the environment.

As an example, in Fig. 6, we show the exhaustively optimized Airy parameter B for each RX location within the marked region, i.e., emulating a fixed obstacle and mobile receiver. We observe that the optimum value of B is highly sensitive to the RX location. More interestingly, there are some correlations between the RX locations and the optimal curving trajectory, although not straightforward for regression

[5]The Fraunhofer distance in this scenario goes up to 240m at 100 GHz.

[6]The brute force search is at the highest resolution our 96-core server can afford in feasible time (step sizes of $\delta B = 0.02$, $\delta f = 2$cm, $\delta\theta = 0.5°$).

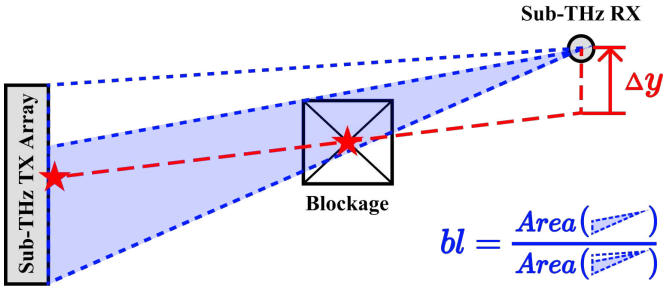

Fig. 7: Illustrating environmental features bl and Δy.

models. Further, such correlation becomes even more complex under blocker mobility. Hence, a deterministic algorithm for Airy beam optimization is not applicable, and a physics-informed neural network is required to understand the complex underlying relationships while considering the laws of diffraction. As mentioned, we implement deterministic near-field beam focusing as a straightforward yet effective baseline for comparison.

B. Preprocessing and Feature Engineering

In order to achieve higher accuracy and faster convergence, we process our dataset to carry more information about the physics of wavefront shaping and offload the burden of blind learning off of the neural network, particularly under limited dataset sizes. We construct two additional environment features bl and Δy as shown in Fig. 7. Specifically, the blockage index bl captures how much the obstacle blocks the LOS path in a given environment. As shown, it is calculated by computing the ratio between the shaded blocked region and the total triangular region that could otherwise be used for beam focusing. bl informs the neural network of the extent of blockage and has an impact on optimal Airy configurations. It also serves as the activation threshold (blockage criteria) in our overall framework shown in Fig. 5: from empirical data, we set the threshold to be $bl_T = 0.75$ (i.e., we activate the neural network only if $bl \geq 0.75$). On the other hand, Δy captures the relative location of the receiver when compared to the TX-obstacle axis. Note that $\Delta y > 0$ when the receiver is above the axis of interest (see Fig. 7), and $\Delta y \leq 0$ if otherwise. Δy plays a vital role in our physics-informed network architecture and the direction of curving. Finally, under each environment, we compute the deterministic beam focusing parameters $\{f_D, \theta_D\}$ and use focal/steering adjustments $\{\Delta f = f - f_D, \Delta\theta = \theta - \theta_D\}$ instead of absolute values $\{f, \theta\}$ as neural network outputs. This helps with faster convergence. As such, we aim to map the 8-dimensional input space $\{O_x, O_y, d_x, d_y, R_x, R_y, bl, \Delta y\}$ to a 3-dimensional output space $\{B, \Delta f, \Delta\theta\}$.

C. Physics-Informed Neural Network

After our feature engineering that highlights the importance of geometric topology, we architect a physics-informed neural network. Here, we use an insight that is rooted in the physics of wave propagation. Specifically, if both the obstacle and RX

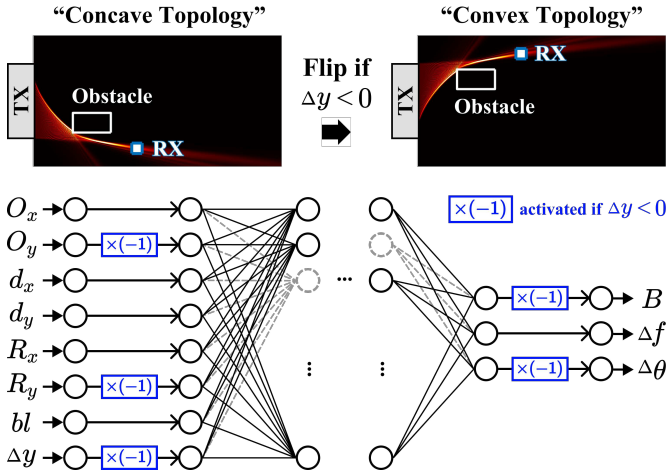

Fig. 8: Topology flipping and physics-informed neural network architecture to guarantee symmetric performance by design.

are mirrored with respect to the perpendicular bisector of the transmitter's array, then the optimal airy beam is mirrored too. As depicted in Fig. 3, if the topology of the environment is flipped along the transverse direction (i.e., $O_y \to -O_y, R_y \to -R_y$), then we can easily find the new optimal Airy beam configuration without any calculation (i.e., $B^\star \to -B^\star, \theta^\star \to -\theta^\star$). This is inherently due to the symmetric nature of the system with respect to $y = 0$.

Hence, we can break down all possible topologies into two distinct and symmetric categories, concave ($\Delta y < 0$) and convex ($\Delta y > 0$) topologies. To facilitate learning of the physical system, we enforce the inherent topological symmetry of the system and train the neural network only on convex topologies. In other words, our neural network only learns to optimize Airy beams for convex cases, while concave cases are handled through geometric symmetry. This further offloads the burden of blind learning from the neural network.

The detailed network design is shown in Fig. 8. Specifically, $\{O_y, R_y, \Delta y\}$ will be flipped in sign if $\Delta y < 0$ in the input environment topology. After hyperparameter tuning, we converge to $4\times$ dense layers with 10% drop-out rate. Finally, if $\Delta y < 0$, the output values of B and $\Delta\theta$ are flipped back to retrieve the final Airy configuration. We perform standardization on both the input and output variables. During the training process, we adopt MAE as the loss function to reduce the impact of outliers and we use SGD with momentum as the optimizer to improve training efficiency.

IV. Performance Evaluation

A. Blind Spot Reduction with Curved Beams

Here, we show that the area of blind spots caused by an obstruction (the area in which the received power is extremely low) can be significantly reduced when the transmitter adopts an Airy beam to reach its destination.

We follow the setup in Fig. 6a, where the receiver is located at several location in the close proximity of an obstacle. At each receiver location, the entire beam space is exhaustively

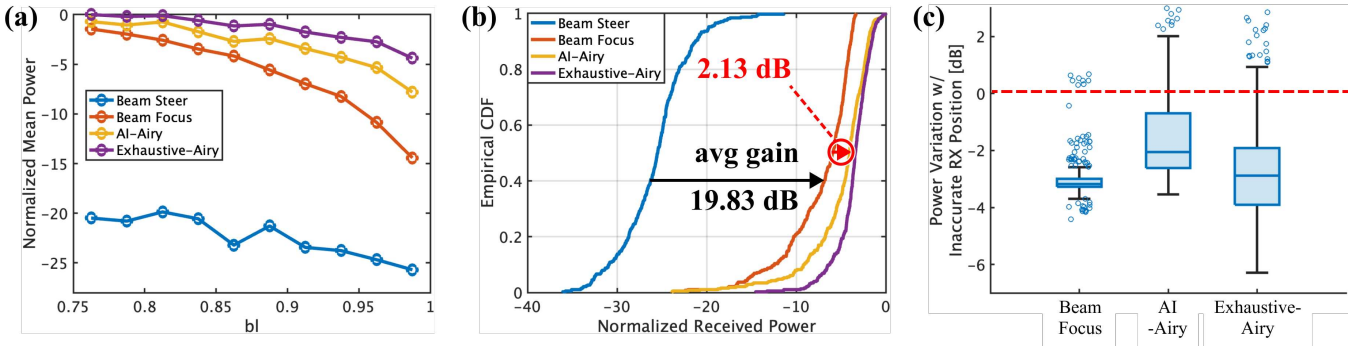

Fig. 9: (a) Comparison of resilience against blockage. (b) Empirical CDF of received power in all simulated environments. (c) Received power variation under imperfect RX location knowledge.

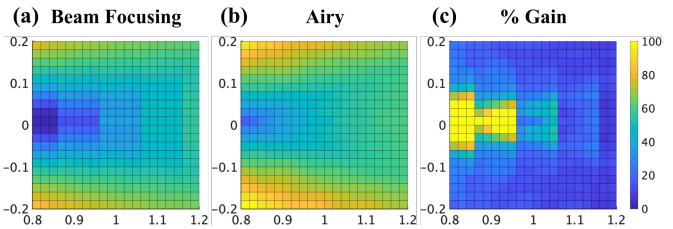

Fig. 10: Blind spot reduction performance. Received power under (a) near-field beam focusing and (b) curved Airy beam. (c) Performance gain (%) in received power from Airy beams.

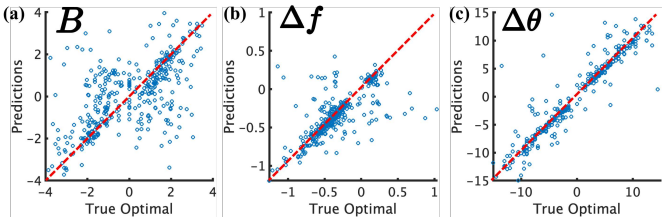

Fig. 11: Parity plots of NN-predicted Airy configurations.

searched with discrete steps to find the true optimal Airy beam configuration $\{B^\star, f^\star, \theta^\star\}$. Comparing the received power maps shown in Fig. 10a and that in Fig. 10b, we see that the shadow region (the dark blue region) is evidently reduced compared with the case in which the transmitter adopts a near-field beam focusing wavefront. We further visualize the gain by calculating the percentage power increase from beam focusing to Airy beams in Fig. 10c, which shows a significant area that sees more than 100% received power improvement. Therefore, Airy Beams (when correctly configured) can indeed provide huge potential for blockage mitigation in sub-THz wireless networks. Yet, an exhaustive scan over the design space to find the right curved beam is not feasible.

B. Accuracy of NN-Predicted Curved Beam

We demonstrate the performance of our Airy optimization framework through extensive simulations, evaluated on a separate test dataset of $\sim$ 400 random blockage environments. Further, we observe consistent learning performance despite random shuffling and splitting between the training and test sets, which confirms the robustness of our framework.

To show the effective learning of our neural network, we show parity plots where the predicted $\{B, \Delta f, \Delta\theta\}$ labels are plotted against the ground truth $\{B^\star, \Delta f^\star, \Delta\theta^\star\}$ labels from exhaustive search (Fig. 11a-c). We observe that a general trend of positive correlation (along $y = x$) can be found in all three parity plots, despite huge variances in environmental configurations and a large number of outlier scenarios (e.g., full blockage, edge diffraction, etc.). We report R^2 scores of 0.31, 0.47, and 0.87 for B, Δf, $\Delta\theta$ predictions, respectively.

Next, we show the performance of our NN-predicted Airy configurations. Specifically in each test scenario, we calculate the received power under *(i)* Conventional far-field beam steering, *(ii)* Near-field beam focusing, *(iii)* AI-predicted Airy configurations, and *(iv)* Exhaustive Airy configurations. Fig. 9a shows normalized mean received powers under each method, grouped by and plotted against the blockage index bl. As expected, as the blockage gets more severe, the received power drops. Nevertheless, we observe that Airy beams maintain a relatively strong SNR despite severe blockage conditions, even compared with near-field beam focusing, showing a unique resilience against channel blockage. Further, it is evident that the NN-predicted Airy configurations are able to achieve near-optimal performances compared to the brute force scheme.

In practice, we envision that the transmitter would adopt a two-shot wavefront selection, i.e., it compares the performance of near-field beam focusing with AI-generated Airy wavefront and locks into the one achieving the higher SNR. We note that calling the pre-trained neural network for prediction induces minimal computational overhead. Further, the amount of time overhead for curved beam configuration is dependent on the computational resources and phase switching speed of the transmitting node. Regardless, this overhead is constant and negligible in practical settings.

The overall power performance of such a method is compared with baselines in Fig. 9b. We observe that AI-generated Airy beams can achieve a significant average gain of 19.83 dB compared with conventional beam steering and 2.13 dB

compared with near-field beam focusing. Again, as shown, the performance of AI-generated curved beams is close to that of the true-optimal wavefronts (average loss of under 0.8 dB compared with the impractical exhaustive search).

So far, we assumed the RX's location is perfectly known. Here, we evaluate the performance under inaccurate RX positioning. In each of the ~ 400 test scenarios, we move the RX within a square-shaped region centered around its true location (R_x, R_y), with a side length of 20cm. We calculate the average received power across these RX locations and compare it with the case where the RX is accurately placed. Fig. 9c plots the received power variation caused by inaccurate RX positioning under different methods. We observe that our AI-enabled framework works the best under receiver uncertainty as compared to beam focusing and brute force optimization. This is because *(i)* the Airy diffraction has larger coverage and *(ii)* compared with beam focusing, our framework takes into account environmental information (other than the receiver locations). Interestingly, inaccurate RX information may yield even higher received power in some instances. We highlight that resilience to RX location errors was not considered when training the neural network. In the future, we will explore AI-based frameworks that take into account both SNR and resilience objectives for Airy beam engineering.

V. Conclusion

To conclude, we present a physics-informed NN-enabled framework for real-time obstacle-avoiding Airy beams in sub-THz wireless systems. We observe that the proposed framework can achieve a 19.83 dB gain from conventional far-field beam steering, and a 2.13 dB gain compared with near-field beam focusing. Our NN-predicted Airy configurations also show interesting resilience against inaccurate RX locations. We believe that, by providing a low-overhead solution for Airy beam optimization, this work paves the way for the adoption of such complex wavefronts in future sub-THz networks.

References

[1] I. F. Akyildiz, C. Han, Z. Hu, S. Nie, and J. M. Jornet, "Terahertz Band Communication: An Old Problem Revisited and Research Directions for the Next Decade," *IEEE Transactions on Communications*, vol. 70, no. 6, pp. 4250–4285, 2022.

[2] A. Kludze and Y. Ghasempour, "LeakyScatter: A Frequency-Agile Directional Backscatter Network above 100 GHz," in *20th USENIX Symposium on Networked Systems Design and Implementation (NSDI 23)*, 2023, pp. 375–388.

[3] J. M. Jornet, E. W. Knightly, and D. M. Mittleman, "Wireless Communications Sensing and Security above 100 GHz," *Nature communications*, vol. 14, no. 1, p. 841, 2023.

[4] S. S. Afzal, A. Kludze, S. Karmakar, R. Chandra, and Y. Ghasempour, "AgriTera: Accurate Non-Invasive Fruit Ripeness Sensing via Sub-Terahertz Wireless Signals," in *Proceedings of the 29th Annual International Conference on Mobile Computing and Networking*, 2023, pp. 1–15.

[5] V. Petrov, M. Komarov, D. Moltchanov, J. M. Jornet, and Y. Koucheryavy, "Interference and SINR in Millimeter Wave and Terahertz Communication Systems with Blocking and Directional Antennas," *IEEE Transactions on Wireless Communications*, vol. 16, no. 3, pp. 1791–1808, 2017.

[6] Z. Chen, B. Ning, C. Han, Z. Tian, and S. Li, "Intelligent Reflecting Surface Assisted Terahertz Communications Toward 6G," *IEEE Wireless Communications*, vol. 28, no. 6, pp. 110–117, 2021.

[7] R. Shen and Y. Ghasempour, "Scattering from Rough Surfaces in 100+ GHz Wireless Mobile Networks: From Theory to Experiments," in *Proceedings of the 29th Annual International Conference on Mobile Computing and Networking*, 2023, pp. 1–15.

[8] A. Singh, V. Petrov, H. Guerboukha, I. V. Reddy, E. W. Knightly, D. M. Mittleman, and J. M. Jornet, "Wavefront Engineering: Realizing Efficient Terahertz Band Communications in 6G and Beyond," *IEEE Wireless Communications*, 2023.

[9] H. Guerboukha, B. Zhao, Z. Fang, E. Knightly, and D. M. Mittleman, "Curving THz Wireless Data Links around Obstacles," *Communications Engineering*, vol. 3, no. 1, pp. 1–8, 2024.

[10] H. Chen, "Dataset and Neural Network Parameters for Airy Beam Optimization, GlobeCom 2024." [Online]. Available: https://github.com/haoze-chen/GlobeCom-Airy

[11] G. Siviloglou, J. Broky, A. Dogariu, and D. Christodoulides, "Observation of Accelerating Airy Beams," *Physical Review Letters*, vol. 99, no. 21, p. 213901, 2007.

[12] J. W. Goodman, *Introduction to Fourier Optics*. Roberts and Company publishers, 2005.

[13] T. Latychevskaia, D. Schachtler, and H.-W. Fink, "Creating Airy Beams Employing a Transmissive Spatial Light Modulator," *Appl. Opt.*, vol. 55, no. 22, pp. 6095–6101, Aug 2016.

[14] C. Han, Y. Wang, Y. Li, Y. Chen, N. A. Abbasi, T. Kürner, and A. F. Molisch, "Terahertz Wireless Channels: A Holistic Survey on Measurement, Modeling, and Analysis," *IEEE Communications Surveys Tutorials*, vol. 24, no. 3, pp. 1670–1707, 2022.

[15] Y. Ghasempour, C. R. Da Silva, C. Cordeiro, and E. W. Knightly, "IEEE 802.11ay: Next-Generation 60 GHz Communication for 100 Gb/s Wi-Fi," *IEEE Communications Magazine*, vol. 55, no. 12, pp. 186–192, 2017.